

Experimental Determination of the ZIP Coefficients for Modern Residential, Commercial, and Industrial Loads

Abdullah Bokhari, *Student Member, IEEE*, Ali Alkan, Rasim Dogan, Marc Diaz-Aguiló, Francisco de León, *Senior Member, IEEE*, Dariusz Czarkowski, *Member, IEEE*, Zivan Zabar, *Senior Member, IEEE*, Leo Birenbaum, *Senior Member, IEEE*, Anthony Noel, *Member, IEEE*, and Resk Ebrahem Uosef, *Member, IEEE*

Abstract—This paper presents the experimental determination of the ZIP coefficients model to represent (static) modern loads under varying voltage conditions. ZIP are the coefficients of a load model comprised of constant impedance Z , constant current I , and constant power P loads. A ZIP coefficient load model is used to represent power consumed by a load as a function of voltage. A series of surveys was performed on typical residential, commercial, and industrial customers in New York City. Household appliances and industrial equipment found in the different locations were tested in the laboratory by varying the voltage from 1.1-p.u. voltage to 0 and back to 1.1 pu in steps of 3 V to obtain the individual P - V , Q - V , and I - V characteristics. Customer load tables were built using seasonal factors and duty cycles to form weighted contributions for each device in every customer class. The loads found in several residential classes were assembled and tested in the lab. It was found that modern appliances behave quite differently than older appliances even from only 10 years back. Models of the different customer classes were validated against actual recordings of load variations under voltage reduction.

Index Terms—Commercial class, industrial class, load characteristic, load composition, load model, residential class, ZIP coefficients.

I. INTRODUCTION

LOAD composition has changed substantially from a few years back. In the last 10 years, the proliferation of power-electronic supplies used in many household loads (for example: flat screen TVs, fluorescent compact lights (CFLs), laptop and cell-phone chargers) has modified substantially the way loads behave as the voltage varies [1]–[3]. The lighting industry has

Manuscript received March 15, 2013; revised August 28, 2013; accepted October 01, 2013. Date of publication October 28, 2013; date of current version May 20, 2014. Paper no. TPWRD-00307-2013.

A. Bokhari, A. Alkan, R. Dogan, M. Diaz-Aguiló, F. de León, D. Czarkowski, Z. Zabar, and L. Birenbaum are with the Department of Electrical and Computer Engineering, Polytechnic Institute of New York University, Brooklyn, NY 11201 USA (e-mail: abdullah.bokhari@gmail.com; rsmdgn marc.diaz.aguilo@gmail.com; aalkan01@students.poly.edu; fdeleon@poly.edu; dcz@poly.edu; zzbar@poly.edu; lbirenba@duke.poly.edu).

A. Noel is with Public Service Electric and Gas Company, Newark, NJ 07102 USA (e-mail: anthony.noel@pseg.com).

R. E. Uosef is with Consolidated Edison Inc., New York, NY 10003 USA (e-mail: uosefr@coned.com).

Color versions of one or more of the figures in this paper are available online at <http://ieeexplore.ieee.org>.

Digital Object Identifier 10.1109/TPWRD.2013.2285096

gone through a significant development in ballast technology, and today electronic ballasts are more popular than magnetic ballasts [1]–[5]. In addition to energy savings, electronic ballasts have constant power consumption under voltage variation, better power regulation, and color consistency. On the other hand, magnetic ballasts behave as constant impedance loads. Similarly, outdoor lighting is driving innovation in high-intensity lighting (HID). Within this segment, there has been a major technology shift from mercury vapor to high-pressure sodium and, finally, to metal halide lights. New types of indoor and outdoor lights are now being introduced to the market as, for example, induction lights and light-emitting diode (LED) lights, which are expected to dominate the lighting industry due to their better energy efficiency [3], [6]–[9].

The objective of this paper is to present a ZIP coefficients model which accurately describes the steady-state behavior of modern loads under varying voltage conditions. An investigation on the effect of varying load is introduced by analyzing individual and composite load structures by means of ZIP coefficients. The work described here is part of a project intended to estimate the impacts of conservation voltage reduction (CVR) for customers and utilities. CVR is a technique commonly used by power utilities to conserve energy by reducing the voltage delivered to the loads. The main idea is that loads (devices, appliances, etc.) consume less power when the applied voltage reduces. Validation of the composite load model and ZIP coefficients against field measurements are presented in [27].

The polynomial expression known as the ZIP coefficients model represents the variation (with voltage) of a load as a composition of the three types of constant loads Z , I , and P . Z , I , and P stand for constant impedance, constant current, and constant power loads, respectively. The expressions for active and reactive powers of the ZIP coefficients model are

$$P = P_0 \left[Z_p \left(\frac{V_i}{V_0} + I_p \frac{V_i}{V_0} + P_p \right) \right] \quad (1)$$

$$Q = Q_0 \left[Z_q \left(\frac{V_i}{V_0} + I_q \frac{V_i}{V_0} + P_q \right) \right] \quad (2)$$

where P and Q are the active and reactive powers at operating voltage (V_i); P_0 and Q_0 are the active and reactive powers at rated voltage (V_0); Z_p , I_p , and P_p are the ZIP coefficients for active power; and Z_q , I_q , and P_q are the ZIP coefficients for reactive power.

TABLE I
SAMPLE SERVICE CLASSES AND THEIR STRATUM CLASSIFICATION

Service Class	Description	Stratum billing variable
SC 1	Residential	Annual kWh
SC 2	Small commercial	June-Sept. kWh
SC 5	Electric traction system	Annual kWh
SC 6	Private street lighting	Month of year
SC 9	Large commercial	Average of June-Sept. kW
SC 12	Multiple dwelling space heating	Nov.-Feb. kWh

The tasks performed to obtain an accurate load model were: 1) field surveys were conducted for a number of residential, commercial, and industrial customers in New York City. From these surveys, information on the composition of their loads was obtained. A list of the most common appliances and devices used in each customer class was made; 2) voltage variation tests (from $1.1 V_{pu}$ to 0, and then from 0 to $1.1 V_{pu}$) were performed in the laboratory on both individual devices, and on composite loads, found for the different customer classes; 3) from these experiments, ZIP coefficient models were built by fitting quadratic functions to the data using a constrained optimization algorithm; and 4) actual recordings of load variation under voltage reduction were compared with results predicted from the models for each customer class.

II. LITERATURE REVIEW

Load modeling and load characterization studies have been performed for a long time. A study performed in 1923 obtained a miniature model for an *ac* network with details of the network components [10]. The study compared the actual system and the miniature model under varying load. A study performed in 1973 addressed composite loads and load parameters and included the effects of feeders and distribution transformers [11]. The voltage and frequency dependency of these composite loads were also investigated.

In 1992, an IEEE Task Force published a paper on "Load Representation for Dynamic Performance Analysis," summarizing the current status on power system load modeling [12]. Definitions of basic load modeling concepts were explained and the importance of further developments in load modeling was discussed. Numerous studies comparing the performance of load modeling have been published (see [12]–[15]). A mathematical expression relating load characteristics to depressed voltage levels by means of the sum of constant impedance (Z), constant current (I), and constant power (P) components, was introduced by Kalinowsky and Forte in 1981 [16]. However, the use of such a linear combination was first introduced by Kent *et al.* in 1969 [17]. The ZIP coefficients model has been widely used to represent the relation between voltage and power characteristics of loads [18], [19].

III. CUSTOMER CLASSES

Load composition of customers plays a significant role in determining the appropriate load model. Load composition varies according to many factors such as the type, size, behavior of the customer, and recent advances and upgrades in equipment technology. In this study, load composition is organized based on the customer class with a recognized load profile.

TABLE II
TYPICAL RESIDENTIAL LOAD STRUCTURE

Equipment	Total No.	Rated Power [kW]	Duty Cycle	Season Factor			Total Power [kWh]		
				Spring	Summer	Winter	Spring	Summer	Winter
TV	1	0.208	1	0.2	1	0.2	0.8	0.6	0.8
PC	1	0.119	1	0.2	0.2	0.2	0.6	0.6	0.6
Laptop Ch.	1	0.036	0.6	0.6	0.4	0.6	0.3	0.2	0.3
Minibar	1	0.091	0.5	1	1	1	1.1	1.1	1.1
Incandescent	1	0.087	1	0.2	0.2	0.2	0.4	0.4	0.5
CFL Bulb	1	0.026	1	0.4	0.3	0.6	0.3	0.2	0.3
Fan	1	0.163	1	0.1	0.1	0	0.4	0.6	0
Air Cond.	1	0.496	1	0.1	0.3	0	1.2	3.9	0
Total							5.02	7.46	3.57
Reported average peak power (weekdays)							5.05	7.40	3.56

A "load component" is here defined as the aggregate equivalent of all devices with similar behavior; for example: electrical heating (ambient and water), motor loads (air conditioners, pumps), and power-electronics loads (fluorescent lights, TVs, chargers). Customers are generally grouped into three major classes: 1) residential; 2) commercial; and 3) industrial; see [20]. In each class, the load consists of the sum of several different "load components," each of which contributes some fraction to the total load; see [21]. As a result, different types and quantities of loads may be connected or disconnected in a power system during a day. It is known that the load composition of each class exhibits different behavior with the change in weather conditions, economical situation, and culture [22], [23].

Three approaches exist for load modeling: measurement-based models, disturbance-based models, and component-based models [24], [25]. For the purpose of this study, the component-based approach is adopted, since it has been widely used in load flow and stability studies; has the advantage of not requiring field measurement; and can be applied to different operating conditions [23].

To implement the component-based approach in this study, customers in New York City were identified based on their load shape for their hourly demand. Load shape depends on: 1) the type of day (weekday or holiday); 2) service class (SC), which represents a group of customer types with similar load characteristics (i.e., residential, small commercial, large commercial, and industrial); 3) stratum: each service class is decomposed into subgroups, or strata, within a service class based on customer size, as measured by a particular billing quantity (details are given below); and 4) temperature. Table I shows samples of service classes with their stratum billing variable.

IV. LOAD SURVEYS

To investigate load profiles of each customer class in a targeted network, surveys were conducted in several sites of the network. This gave an accurate estimation of load composition. Onsite visits were performed on different customer classes, and information on the details of each customer load was recorded. The surveys were aimed to obtain the nature of loads in each customer class, the electrical data, the total number of equipment being used, and how often those pieces of equipment were

TABLE III
CLASSIFICATION OF RESIDENTIAL STRATA BASED ON ANNUAL CONSUMPTION

Residential strata	Annual low bound [kWh]	Annual high bound [kWh]
A	0	1948
B	1948	2897
C	2897	3897
D	3897	5239
E	5239	7741
F	7741	

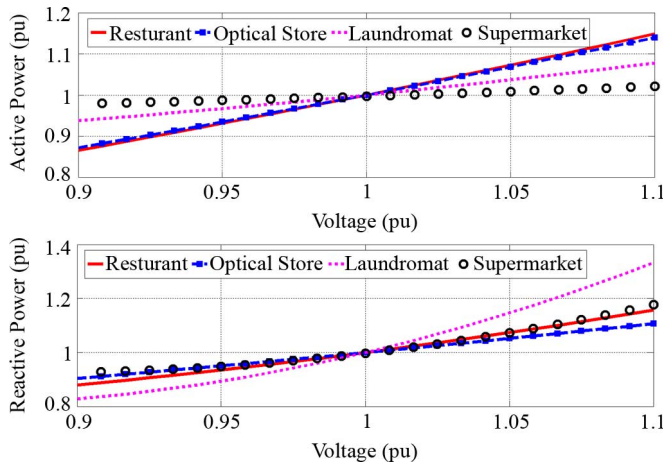


Fig. 1. Reconstructed active and reactive power curves for small commercial customers. These power curves use the ZIPs coefficients obtained with actual cutoff voltage reported in the second half of Table VII.

TABLE IV
EQUIPMENT CONTRIBUTION FOR HIGH SCHOOL AND HOTEL

School load	Weight [%]			Hotel load	Weight [%]		
	Spring	Summer	Winter		Spring	Summer	Winter
Air Comp. 3ph	25.8	24.7	5.68	Air Comp. 3ph	25.8	24.7	5.68
PC3.	3.21	2.02	3.53	Air Comp. 1ph	4.75	6.48	22.3
Copier	2.39	1.15	2.64	Minibar	16.3	16.7	11.5
Projector	0.63	0.33	0.86	Vacuum	0.39	0.59	0.41
Laptop Charger	4.91	3.26	5.41	Coffee Maker	1.36	1.39	9.06
LCD TV	2.83	2.61	3.73	LCD TV	0.11	0.11	0.16
E. Ballast	20.2	19.3	37.8	E. Ballast	2.99	2.99	2.15
Inc. Light	3.03	1.93	4.45	Inc. Light	0.14	0.14	0.1
Heater	0.73	0	3.23	Heater	0.47	43.5	3.33
Refrigerator	0.66	0.35	0.57	Refrigerator	1.95	2	1.38
Fan	9.85	15.7	3.62	Fan	4.6	5.24	6.04
Motor	25.8	28.7	28.5	Elevator	5.29	6.62	6.8
Total	100	100	100	Meta l Halide	2.7	2.5	1.91
				LED Bulb	0.04	0.04	0.02
				Halogen Light	0.05	0.05	0.04
				CFL Light	5.87	5.74	4.32
				Microwave	1.25	2.53	8.69
				Total	100	100	100

connected or disconnected during the day. In addition, the behavior of each load class varies with the change of weather, type of activity, and economic situation. Survey data provided guidance for the selection of the equipment to test in the laboratory.

The survey data, for a service class, were extracted and categorized based on equipment characteristics. The types of loads observed during the surveys fall into the following categories:

- lighting equipment: fluorescent, incandescent, halogen, compact fluorescent lights (CFL), and high-intensity discharge (HID) lights;

- elevators: hydraulic, pneumatic, and traction;
- air handling: HVAC, chillers, fans, and heat pumps;
- pumps: hot and cold water circulation, chiller pumps, fire pumps, and centrifugal pumps;
- compressors: air compressors and industrial freezers;
- household appliances: refrigerators, freezers, warmers, ovens, and microwaves;
- power-electronics devices: power supplies, chargers, TVs, game consoles, computers, and peripherals.

For the purpose of creating an accurate customer load model, each customer load was classified based on running load versus annual load. Since running loads change depending on the temperature, seasons were chosen according to the climate of New York City. Load tables for every surveyed customer were formed into seasonal results. Since climate and energy consumption are closely coupled, each customer class was formed with three seasons: spring/fall, summer, and winter, as loads and consumption vary depending on the season. Spring and fall seasons were combined together, since there is no significant difference between them.

Using the survey information, load tables were built with load component information for every season. Each load component was correlated with a duty cycle, and with a seasonal use factor, since loads do not run all of the time, and their characteristics vary. The total seasonal energy consumption was computed by summing the correlated load component power consumptions. This was done in order to build an accurate detailed load model for each class, taking into account climate change, energy consumption, and the running loads during a season. The load tables so obtained were validated by comparing the calculated hourly power consumption with utility records of hourly energy consumption for a whole year for every surveyed customer. Consumption reports are divided based on defined seasons, and the average hourly peak load for every season was formed. Seasons are defined as follows: spring/fall: March, April, May, June, October, and November; summer: July, August, and September; winter: December, January, and February. The energy consumption for every season matched very well with the actual seasonal average peak kilowatt-hours for the surveyed customers. The constructed load table for a typical residential customer is shown in Table II.

In Table II, the duty cycle indicates the relative time that the equipment is connected. Season factor indicates the relative time that the equipment is in use. Season factor varies as load configuration changes with season (spring/fall, summer, and winter). Both season factor and duty cycle are fractions of a 24-h period, and have a value between 1 and 0.

The actual power of a single item of equipment, and the total component power in a class, is calculated as

$$\begin{aligned} \text{Actual equipment power} &= (\text{equipment rated power}) \\ &\quad \times (\text{duty cycle}) \times (\text{season factor}) \end{aligned} \quad (3)$$

$$\begin{aligned} \text{Total component power} &= (\text{actual equipment power}) \\ &\quad \times (\text{Total number of equipment}). \end{aligned} \quad (4)$$

TABLE V
EQUIPMENT CONTRIBUTION WEIGHT IN% PER CLASS (SUMMER)

Load component/ characteristic	Sub-class A	Sub-class B	Sub-class C	Sub-class D	Sub-class E	Sub-class F	Small commercial	Large commercial	Industrial
Air Conditioner	53.06	57.24	68.19	58.42	32.1	53.07	0	0	0.4
Refrigerator	0	11.89	8.83	6.28	6.9	5.01	4.32	0.34	0
Minibar	14.68	0	0	0	0	0	0.05	0	0
Air Compressor 1ph	0	0	0	0	0	0	0	0	0
Air Compressor 3ph	0	0	0	0	0	0	73.35	23.81	14.81
Fan	7.4	0	0	4.29	11.88	8.19	0.25	15.17	1.66
Vacuum Cleaner	0	0	0	2.25	2.47	1.08	0	0	0
Elevator	0	0	0	0	0	0	1.61	31.12	75.55
CFL Bulb	2.25	5.2	5.85	4.77	8.24	5.33	0	1.87	0.03
Incandescent Bulb	5.37	9.53	7.1	8.88	12.59	10.96	0	0	0
Halogen Bulb	0	0	0	0	0	0	0	0	0
LED Bulb	0	0	0	0	0	0	0	0	0
Electronic Ballast	0	0	0	1.55	2.04	1.48	16.49	18.64	3.92
Magnetic Ballast	0	0	0	0	0	0	0	0	0
Laptop Charger	2.79	1.93	1.59	2.27	2.49	2.27	2.09	3.15	0
PC	7.7	4.73	4.04	2.5	3.43	2.49	0.78	1.95	0.11
Television	6.75	8.27	3.68	4.37	12.01	6.02	0	2.52	0.03
Game Console	0	1.21	0.72	0.83	1.12	0.66	0	0	0
Projector	0	0	0	0	0	0	0	0.32	0
Copier	0	0	0	0	0	0	1.06	1.11	0.08
Kettle	0	0	0	0	0	0	0	0	0
Microwave Oven	0	0	0	3.59	4.73	3.44	0	0	0
Coffee Maker	0	0	0	0	0	0	0	0	0
Metal Halide Eballast	0	0	0	0	0	0	0	0	0
Metal Halide Mballast	0	0	0	0	0	0	0	0	2.46
High Pressure Sodium Mballast	0	0	0	0	0	0	0	0	0.95
Mercury Vapor Light	0	0	0	0	0	0	0	0	0
Induction Light	0	0	0	0	0	0	0	0	0
Tungsten Light	0	0	0	0	0	0	0	0	0

TABLE VI
ACTIVE AND REACTIVE ZIP MODEL PER CUSTOMER CLASS (SUMMER)

Customer class	Z_p	I_p	P_p	Z_q	I_q	P_q
Residential	stratum A	1.5	-2.31	1.81	7.41	-11.97
	stratum B	1.57	-2.48	1.91	9.28	-15.29
	stratum C	1.56	-2.49	1.93	10.1	-16.75
	stratum D	1.31	-1.94	1.63	9.2	-15.27
	stratum E	0.96	-1.17	1.21	6.28	-10.16
	stratum F	1.18	-1.64	1.47	8.29	-13.67
Small commercial	Duane Reade	0.27	-0.33	1.06	5.48	-9.7
	5Guys Burger	0.69	0.04	0.27	1.82	-2.24
	Laundromat	0.77	-0.84	1.07	8.09	-13.65
	Optics	0.55	0.24	0.21	0.55	-0.09
Large commercial	School	0.4	-0.41	1.01	4.43	-7.98
	Hotel	0.76	-0.52	0.76	6.92	-11.75
Industrial		1.21	-1.61	1.41	4.35	-7.08

Notes: 1) Normalized active power (P_0), reactive power (Q_0), and voltage (V_0) are equal to 1 (in pu); 2) Cutoff voltage (V_{cut}) for all classes equal to 100 V. The customer class ZIPS shown in this table use the devices ZIPS obtained with actual cut-off voltage reported in the second half of Table VII.

Authorized licensed use limited to: Hohai University Library. Downloaded on January 19, 2026 at 16:07:36 UTC from IEEE Xplore. Restrictions apply.

A. Residential Customers

Surveys were performed on different size dwellings (ranging from studio apartments to a large house) to determine, in detail, which household appliances were used in each dwelling. This information was used to construct a set of residential load tables depending on the size and power consumption of the residential unit.

Consolidated Edison Inc (the utility company of New York City) classifies the residential class into six subclasses (or strata) A, B, C, D, E, and F based on annual peak power consumption records; see Table III.

B. Commercial Customers

Commercial sites are designated as either “large” or “small” by Consolidated Edison. Each of these two groups is divided into different subclasses, according to their annual peak power, as for the residential subclasses. Surveys were conducted of four small commercial businesses: a supermarket; a restaurant; a laundromat; and an optical store. Also, two large commercial establishments (a school and a hotel) were surveyed.

TABLE VII
ACTIVE AND REACTIVE ZIP MODEL. FIRST HALF OF THE ZIPS WITH 100-V CUTOFF VOLTAGE.
SECOND HALF REPORTS THE ZIPS WITH ACTUAL CUTOFF VOLTAGE

Equipment/ component	No. tested	V_{cut}	V_o	P_o	Q_o	Z_p	I_p	P_p	Z_q	I_q	P_q
Air compressor 1 Ph	1	100	120	1109.01	487.08	0.71	0.46	-0.17	-1.33	4.04	-1.71
Air compressor 3 Ph	1	174	208	1168.54	844.71	0.24	-0.23	0.99	4.79	-7.61	3.82
Air conditioner	2	100	120	496.33	125.94	1.17	-1.83	1.66	15.68	-27.15	12.47
CFL bulb	2	100	120	25.65	37.52	0.81	-1.03	1.22	0.86	-0.82	0.96
Coffeemaker	1	100	120	1413.04	13.32	0.13	1.62	-0.75	3.89	-6	3.11
Copier	1	100	120	944.23	84.57	0.87	-0.21	0.34	2.14	-3.67	2.53
Electronic ballast	3	100	120	59.02	5.06	0.22	-0.5	1.28	9.64	-21.59	12.95
Elevator	3	174	208	1381.17	1008.3	0.4	-0.72	1.32	3.76	-5.74	2.98
Fan	2	100	120	163.25	83.28	-0.47	1.71	-0.24	2.34	-3.12	1.78
Game consol	3	100	120	60.65	67.61	-0.63	1.23	0.4	0.76	-0.93	1.17
Halogen	3	100	120	97.36	0.84	0.46	0.64	-0.1	4.26	-6.62	3.36
High pressure sodium HID	4	100	120	276.09	52.65	0.09	0.7	0.21	16.6	-28.77	13.17
Incandescent light	2	100	120	87.16	0.85	0.47	0.63	-0.1	0.55	0.38	0.07
Induction light	1	100	120	44.5	4.8	2.96	-6.04	4.08	1.48	-1.29	0.81
Laptop charger	1	100	120	35.94	71.64	-0.28	0.5	0.78	-0.37	1.24	0.13
LCD Television	1	100	120	208.03	-20.58	0.11	-0.17	1.06	1.58	-1.72	1.14
LED light	1	100	120	3.38	5.85	0.58	1.13	-0.71	1.78	-0.8	0.02
Magnetic ballast	1	100	120	81.23	8.2	-1.58	3.79	-1.21	36.18	-67.78	32.6
Mercury vapor HID light	2	100	120	268.27	77.66	0.52	1.02	-0.54	-1.33	2.4	-0.07
Metal halide HID electronic ballast	2	100	120	113.7	26.37	1	-2.02	2.02	8.8	-18.64	10.84
Metal halide HID magnetic ballast	2	100	120	450	102.94	0.86	-0.66	0.8	32.54	-59.83	28.29
Microwave	2	100	120	1365.53	451.02	1.39	-1.96	1.57	50.07	-93.55	44.48
Minibar	1	100	120	90.65	126.94	2.5	-4.1	2.6	2.56	-2.76	1.2
PC (Monitor & CPU)	1	100	120	118.9	172.79	0.2	-0.3	1.1	0	0.6	0.4
Projector	1	100	120	253	44	0.23	-0.52	1.29	0.24	-0.17	0.93
Refrigerator	1	100	120	119.55	52.47	1.17	-1.83	1.66	7.07	-10.94	4.87
Resistive heater	1	100	120	914.78	1.46	0.64	0.59	-0.23	0.13	0.75	0.12
Tungsten light	1	100	120	256.2	21.04	0.43	0.7	-0.13	-0.11	0.66	0.45
Vaccum	1	100	120	855	221	1.18	-0.38	0.2	4.1	-5.87	2.77
Air compressor 1 Ph	1	25	120	1109.01	487.08	0.73	0.38	-0.11	0.45	0.51	0.04
Air compressor 3 Ph	1	79	208	1168.54	844.71	1.16	-1.81	1.65	3.58	-5.25	2.67
Air conditioner	2	75	120	496.33	125.94	1.6	-2.69	2.09	12.53	-21.11	9.58
CFL bulb	2	55	120	25.65	37.52	-0.63	1.66	-0.03	-0.34	1.4	-0.06
Coffeemaker	1	57	120	1413.04	13.32	0.98	0.03	-0.01	0.84	-0.3	0.46
Copier	1	48	120	944.23	84.57	0.52	0.45	0.03	0.39	-0.25	0.86
Electronic ballast	3	95	120	59.02	5.06	-0.07	0.08	0.99	9.32	-20.96	12.64
Elevator	3	110	208	1381.17	1008.3	2.36	-4.15	2.79	11.69	-19.5	8.81
Fan	2	20	120	163.25	83.28	0.26	0.9	-0.16	0.5	0.62	-0.12
Game consol	3	66	120	60.65	67.61	0.36	-0.58	1.22	0.34	-0.12	0.78
Halogen	3	20	120	97.36	0.84	0.51	0.55	-0.05	0.43	0.52	0.05
High pressure sodium HID	4	62	120	276.09	52.65	-0.16	1.2	-0.04	3.26	-4.11	1.85
Incandescent light	2	20	120	87.16	0.85	0.54	0.5	-0.04	0.46	0.51	0.03
Induction light	1	78	120	44.5	4.8	0.18	-0.75	1.57	7.51	-12.35	5.84
Laptop charger	1	46	120	35.94	71.64	0.25	-0.48	1.23	0.14	0.32	0.54
LCD Television	1	73	120	208.03	-20.58	0.33	-0.57	1.24	19	-33.22	15.22
LED light	1	81	120	3.38	5.85	0.69	0.92	-0.61	1.84	-0.91	0.07
Magnetic ballast	1	91	120	81.23	8.2	-3.16	6.85	-2.69	34.26	-64.04	30.78
Mercury vapor HID light	2	88	120	268.27	77.66	-0.16	2.33	-1.17	0.42	-1.01	1.59
Metal halide HID electronic ballast	2	80	120	113.7	26.37	-0.03	-0.06	1.09	11.4	-23.5	13.1
Metal halide HID magnetic ballast	2	47	120	450	102.94	-0.2	1.35	-0.15	1.37	-0.63	0.26
Microwave	2	85	120	1365.53	451.02	-0.27	1.16	0.11	15.64	-27.74	13.1
Minibar	1	58	120	90.65	126.94	3.95	-6.46	3.51	4.84	-6.64	2.8
PC (Monitor & CPU)	1	63	120	118.9	172.79	0.18	-0.26	1.08	-0.19	0.96	0.23
Projector	1	66	120	253	44	0.19	-0.45	1.26	10.18	-18.01	8.83
Refrigerator	1	60	120	119.55	52.47	5.03	-8.48	4.45	17.44	-28.62	12.18
Resistive heater	1	20	120	914.78	1.46	0.92	0.1	-0.02	0.15	0.86	-0.01
Tungsten light	1	27	120	256.2	21.04	0.45	0.66	-0.11	0.21	0.11	0.68
Vaccum	1	20	120	855	221	0.92	0.07	0.01	0.91	-0.02	0.11

Detailed information was obtained. Load tables for each commercial customer were built and the total energy consumption

was computed. Utility records of annual consumption with hourly recordings for each surveyed location exist. Comparison

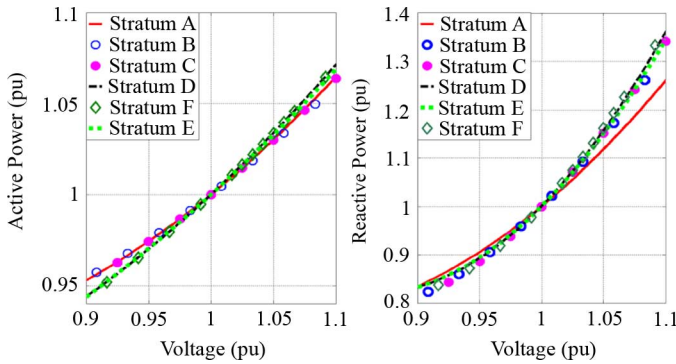


Fig. 2. Residential strata constructed active (left) and reactive (right) power curves. These power curves are using the ZIPs coefficients obtained with actual cutoff voltage reported in the second half of Table VII.

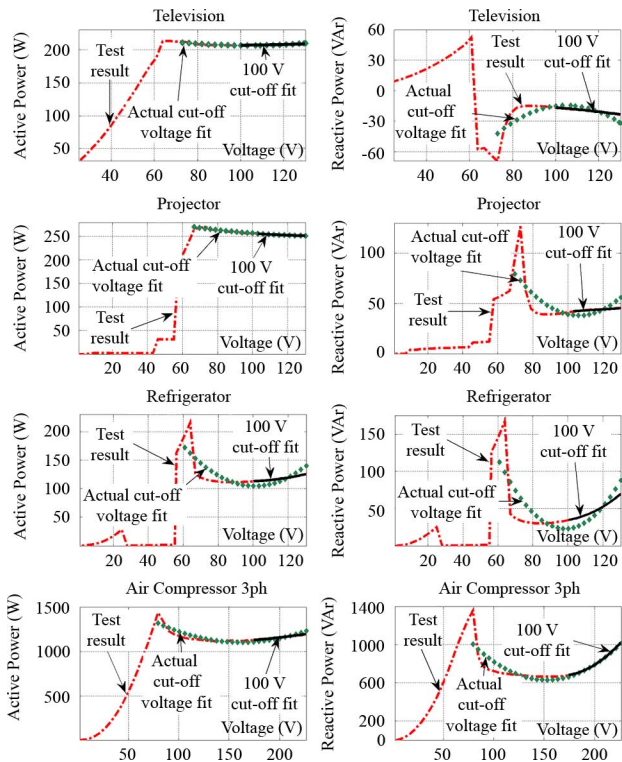


Fig. 3. Active and reactive test results with constrained curve fitting. The ZIP curve with the 100-V cutoff is shown in the solid line and ZIP with the actual cutoff voltage in the dashed line. The two sets of ZIPs are shown in Table VII.

of these records with computed power consumption for each season showed very good agreement.

1) Small Commercial Customers: Commercial customers vary depending on the type of load used by them to conduct their business activities. For example, laundromat loads are mostly motor driven, while the load of a restaurant is primarily resistive. The selection of surveyed customers included businesses with: an HVAC system with resistive heating; a centralized ac system with gas heating, and a normal air conditioning system. This was done in order to ensure a complete investigation of the small commercial class.

Fig. 1 shows how active and reactive powers vary for each surveyed customer. Customers having mainly constant impedance equipment (i.e., restaurant and optical store) have

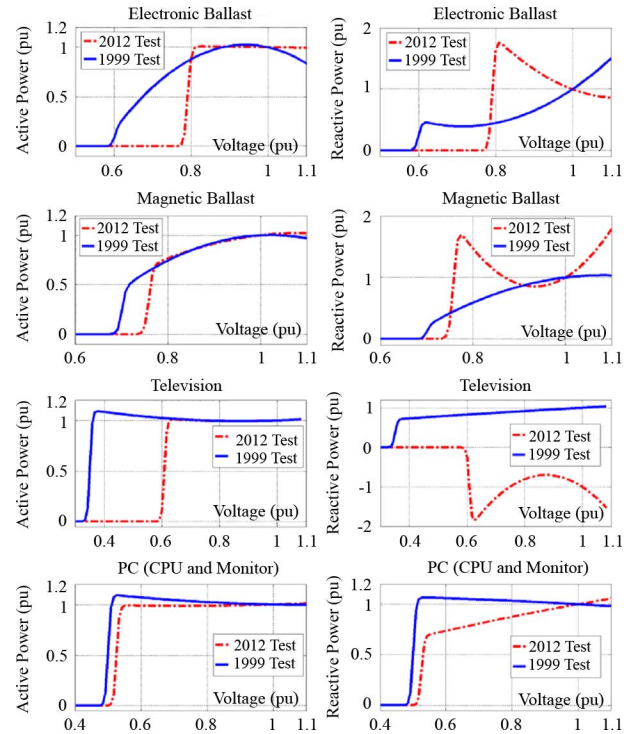


Fig. 4. Comparison of active and reactive powers between old and new appliances.

a higher variation of active and reactive power under voltage reduction. The supermarket load is dominated by the HVAC system with a constant power load behavior. The laundromat almost has a constant current load model. Load topology of a small commercial class varies depending on their type of business activity and their location in New York City. These different load combinations were used to define multiple small commercial classes with a weighted percentage given to each customer load table in order to create a general small commercial load model. A formula for computing small commercial class ZIP coefficients is provided below; see (7)

2) Large Commercial Customers: Load tables for those surveys were constructed and checked against utility records of the average consumption for the three seasons. Table IV shows the percent contribution of equipment for the two customers under study.

Customers in this class have high energy demand and different load behavior depending on the type of business. In general, to fully represent loads in this category, public as well as private customers should be included in the survey. In addition, heating, cooling, and street lighting loads largely contribute in this class, but may differ because of building structure and construction year. To take into account the different customer load compositions in this class, an electrically heated customer (hotel) and a gas-heated customer (high school) were surveyed.

C. Industrial Customers

Two large industrial customers were surveyed. One is a pipeline transportation and energy storage customer and the other is a water treatment plant. Most of the loads found in the

plants are motor-driven pumps and compressors. The collected load information for the power plants was used to formulate the load table and to compute equipment weight. The total calculated energy consumption matched utility records of the average seasonal peak in the annual metered demand.

In general, equipment weight percentages and class ZIP coefficients were calculated as follows:

$$\text{Equipment weight\%} = \left(\frac{\sum \text{load component power}}{\text{class power}} \right) \times 100 \quad (5)$$

$$\text{ZIP}_{\text{residential}} = \sum_{i=A}^F (\text{ZIP}_{\text{stratum}(i)} \times \text{weight}_{\text{stratum}(i)}) \quad (6)$$

$$\text{ZIP}_{\text{small commercial}} = \sum_{i=\text{supermarket, restaurant, laundromat, optical}} (\text{ZIP}_{(i)} \times \text{weight}_{(i)}) \quad (7)$$

$$\text{ZIP}_{\text{large commercial}} = \sum_{i=\text{school, hotel}} (\text{ZIP}_{(i)} \times \text{weight}_{(i)}). \quad (8)$$

Equipment contribution weight in percent per class is shown in Table V for the summer season and the ZIP model per customer class in Table VI.

V. EXPERIMENTS

The setup for the laboratory experiments consisted of a power source, a power analyzer, and computer software. These three elements were used in automated testing to perform tests under identical conditions so that reliable results would be obtained. Voltage reduction tests were performed on each device, and the behavior of these loads was recorded. Prior to each test, loads were operated under nominal voltage in steady state for 30 min to avoid the transient behavior of the cold start. Then, the voltage was decreased from 130 to 0 V in steps of 3 V and kept for 20 s at each step. A settling down period was allowed at each voltage step to prevent any undesired transient. For each step, voltage (V_{rms}), current (I_{rms}), active power (P), and reactive power (Q) were recorded.

A. Isolated Appliances and Equipment

To create a load profile for each surveyed customer, the effect of varying load demand on equipment was investigated. Laboratory experiments were performed on single-phase and on three-phase loads. For several of these tests, loads were built in order to simulate real operating conditions. In most cases, the actual device was used for the test. However, some of the motor loads were emulated. For example, a water pump system was constructed using a centrifugal pump connected to a storage tank through pipes; then pressure was applied using valves. The operation of elevators was emulated with an induction motor

and a controllable dynamometer was controlled to offer constant torque.

During the voltage reduction procedure, loss of load functionality determined the cutoff voltage (V_{cutoff}). We noted, however, that some pieces of equipment continued to consume reactive power even when no work was delivered; examples are induction motors and air compressors. Other loads, such as ballasts and LCD TVs, did not fully stop working, but manifested fluctuations. These experiments provided the correlation between voltage and power (active and reactive) of those loads. The recorded data that fell into the range between 100 to 130 V were used for the curve-fitting process. This is so because the final objective of the project is to assess the load behavior for conservation of voltage reduction studies. Table VII shows the equipment tested in the lab and the generated ZIP coefficients.

B. Assembled Customer Classes

By using the survey information, several customer class loads were reconstructed in the laboratory. Residential strata A, B, C, and D were assembled and voltage reduction tests were performed following the same procedure used for isolated appliances. To ensure the accuracy of customer models, the assembled load composition test results were compared with the reconstructed load shape of the strata. The reconstruction process started with the calculation of active power (P) and reactive power (Q) demand for each appliance used in the particular residential load under study. Next, active and reactive powers were calculated for each load. A simple calculation of the active and reactive powers as a function of voltage for an LCD television is shown in the following equation:

$$P_{tv}(V_i) = 208 \left[0.11 \left(\frac{V_i}{121} \right)^2 - 0.17 \left(\frac{V_i}{121} \right) + 1.06 \right] \quad (9)$$

$$Q_{tv}(V_i) = (-21) \left[1.58 \left(\frac{V_i}{121} \right)^2 - 1.72 \left(\frac{V_i}{121} \right) + 1.14 \right] \quad (10)$$

where V_i is the input voltage and varies from 130 to 100 V in steps of 3 V.

Then, the sum of active and reactive powers for each appliance in the load table was calculated with

$$P_{\text{reconstructed}}(V_i) = P_{rmtv}(V_i) + P_{\text{charge}}(V_i) + \dots + P_{\text{ac}}(V_i). \quad (11)$$

$$Q_{\text{reconstructed}}(V_i) = Q_{tv}(V_i) + Q_{\text{charge}}(V_i) + \dots + Q_{\text{ac}}(V_i). \quad (12)$$

Then, active and reactive power curves were plotted and compared with measurements of the assembled load composition tests. Fig. 2 shows the reconstructed active and reactive power curves using the computed ZIP coefficients for different residential strata.

VI. CALCULATION OF ZIP COEFFICIENTS

A. Method

To obtain this model, for each appliance, active power and reactive power for different voltage levels were measured (see Fig. 3).

B. Calculation of Parameters

If the equipment is a three-phase load, the nominal voltage (V_0) for the fit is set to 208 V. On the other hand, if the load is a single-phase load, the nominal voltage is set to 120 V. To obtain the values of P_0 and Q_0 corresponding to 120 V or 208 V, we performed a preliminary least-square fit in the nominal voltage region ($+/-3$ V). To increase the accuracy of the modeling procedure, a constrained least square was introduced with an optimization routine implemented to deliver the best fit with the constraint that the sum of the three ZIP coefficients has to add to 1. The optimization problem is formulated as follows:

$$\min \left[P_{\text{meas}} - P_0 \left(Z_p \left(\frac{V_i}{V_0} \right)^2 + I_p \left(\frac{V_i}{V_0} \right) + P_p \right) \right]^2 \quad (13)$$

$$\text{Subject to } Z_p + I_p + P_p = 1 \quad (14)$$

and

$$\min \left[Q_{\text{meas}} - Q_0 \left(Z_q \left(\frac{V_i}{V_0} \right)^2 + I_q \left(\frac{V_i}{V_0} \right) + P_q \right) \right]^2. \quad (15)$$

$$\text{Subject to } Z_q + I_q + P_q = 1. \quad (16)$$

Fig. 3 shows active and reactive power curves of the voltage reduction tests for selected pieces of equipment. The figure also shows the corresponding fitted curves obtained between 100 and 130 V (to cover the range for CVR studies) and between the actual cutoff voltage and 130 V to be used for other studies; for example, cold-load pickup studies.

C. Comparison Between Old and New Loads

A study similar to the one described here was performed in 1999 for Consolidated Edison for different appliances and to determine residential and commercial models as static loads [26]. Due to the rapid change in technology, load models needed to be updated to account for the variation of power system load characteristics. A comparison is now presented between the new results and those of the previous study to see how the behavior of modern loads differs from that of older loads.

Fig. 4 shows a comparison of selected appliances; one can note important differences. Within the past decade, electronic ballasts with their constant power behavior replaced magnetic ballasts that follow a constant current curve. New electronic ballast technology has significantly improved from 10 years ago with a better active power regulation over a variety of input voltages. One of the most important characteristics of new electronic ballast circuits is the degree to which they control the lamp power with changes in input voltage. Tests show that new electronic ballasts consume constant active power between 1.1

V_{pu} and 0.8 V_{pu} input voltage. The behavior of reactive power for magnetic and electronic ballasts has also changed as old ballasts resembled constant current loads while the reactive power of new ballasts tends to increase or decrease depending on the supplied voltage level.

With the fast growth of switching power supplies used in LCD TVs and laptop chargers, the consumption and behavior differ from old appliances (CRT TVs). Some appliances today are equipped with power factor correction; for example, the LCD TVs have a slightly leading power factor. By comparing tests of the CRTs from the old study with the new test for the LCD TV, one can see that the reactive power behaves quite differently. Most of the compared appliances indicate that major changes have occurred in their active and reactive power behavior. The study shows that it is essential to update the model for appliances to obtain the correct analysis and design of the network.

VII. CONCLUSION

The paper has presented experimentally verified ZIP coefficient models for the most commonly used appliances and for different customer classes. Surveys were performed to determine which appliances and pieces of equipment were available in the different dwellings and businesses in New York City. The loads found in several residential classes were assembled and tested in the lab. It was found that modern appliances behave quite differently than older appliances even from 10 years ago. The model of the different customer classes has been validated against actual recordings of load variations under voltage reduction in several networks served by Con Edison.

REFERENCES

- [1] K. P. Schneider, J. C. Fuller, and D. P. Chassin, "Multi-state load models for distribution system analysis," *IEEE Trans. Power Syst.*, vol. 26, no. 4, pp. 2425–2433, Nov. 2011.
- [2] F. L. Quilumba, W. Lee, H. Huang, D. Y. Wang, and R. L. Szabados, "Load model development for next generation appliances," in *Proc. Ind. Appl. Soc. Annu. Meeting*, 2011, pp. 1–7.
- [3] B. Zhao, Y. Tang, W. Zhang, and Q. Wang, "Modeling of common load components in power system based on dynamic simulation experiments," in *Proc. Int. Conf. Power Syst. Technol.*, 2010, pp. 1–7.
- [4] Calif. Energy Comm., "2008 building energy efficiency standards for residential and nonresidential buildings," Sacramento, CA, USA, Rep. no. CEC-400-2008-001-CMF, Dec. 2008.
- [5] U.S. Dept. Energy, "CFL market profile: Data trends and market insights," Silver Spring, MD, USA, Sep. 2010, D&R International Ltd.
- [6] Philips Advance, "Pocket guide to high intensity discharge lamp ballasts, Philips lighting electronics," Rosemont, IL, USA, RT-8100-R02 12/09, 2009.
- [7] C. Dilouie, What's New in HID Lamps and Ballasts, Jul. 17, 2012. [Online]. Available: <http://lightingcontrolsassociation.org/whats-new-in-hid-lighting/>
- [8] W. Yan, S. Y. R. Hui, and H. Chung, "Energy saving of large-scale high-intensity-discharge lamp lighting networks using a central reactive power control system," *IEEE Trans. Ind. Electron.*, vol. 56, no. 8, pp. 3069–3078, Aug. 2009.
- [9] "Standard load models for power flow and dynamic performance simulation," *IEEE Trans. Power Syst.*, vol. 10, no. 3, pp. 1302–1313, Aug. 1995.
- [10] O. R. Schurig, "A miniature A-C. transmission system for the practical solution of networks and transmission-system problems," *Trans. Amer. Inst. Electr. Eng.*, vol. 42, pp. 831–840, Jun. 1923.
- [11] G. J. Berg, "Power-system load representation," *Proc. Inst. Elect. Eng.*, vol. 120, no. 3, pp. 344–348, 1973.
- [12] "Load representation for dynamic performance analysis of power systems," *IEEE Trans. Power Syst.*, vol. 8, no. 2, pp. 472–482, May 1993.

- [13] Y. Li, D. Chiang, B. K. Choi, Y. T. Chen, D. H. Huang, and M. G. Lauby, "Representative static load models for transient stability analysis: Development and examination," *Proc. Inst. Elect. Eng., Gen., Transm. Distrib.*, vol. 1, no. 3, pp. 422–431, May 2007.
- [14] A. P. Alves da Silva, C. Ferreira, A. C. Zambroni de Souza, and G. L. Torres, "A new constructive ANN and its application to electric load representation," *IEEE Trans. Power Syst.*, vol. 12, no. 4, pp. 1569–1575, Nov. 1997.
- [15] M. Sadeghi and G. A. Sarvi, "Determination of ZIP parameters with least squares optimization method," in *Elect. Power Energy Conf.*, 2009, pp. 1–6.
- [16] S. A. Kalinowsky and M. N. Forte, "Steady state load-voltage characteristic field tests at area substations and fluorescent lighting component characteristics," *IEEE Trans. Power App. Syst.*, vol. PAS-100, no. 6, pp. 3087–3094, Jun. 1981.
- [17] M. H. Kent, W. R. Schmus, F. A. Mccrackin, and L. M. Wheeler, "Dynamic modeling of loads in stability studies," *IEEE Trans. Power App. Syst.*, vol. PAS-88, no. 5, pp. 756–763, May 1969.
- [18] L. M. Hajagos and B. Danai, "Laboratory measurements and models of modem loads and their effect on voltage stability studies," *IEEE Trans. Power Syst.*, vol. 13, no. 2, pp. 584–592, May 1998.
- [19] S. J. Ranade, A. Ellis, and J. Mechenbier, "The development of power system load models from measurements," in *Proc. Transm. Distrib. Conf. Expo.*, 2001, vol. 1, pp. 201–205.
- [20] E. Vaahedi, M. A. El-Kady, J. A. Libaque-Esaine, and V. F. Carvalho, "Load models for large-scale stability studies from end-user consumption," *IEEE Trans. Power Syst.*, vol. 2, no. PWRS-4, pp. 864–870, Nov. 1987.
- [21] W. W. Price, K. A. Wirgau, A. Murdoch, J. V. Mitsche, E. Vaahedi, and M. El-Kady, "Load modeling for power flow and transient stability computer studies," *IEEE Trans. Power Syst.*, vol. 3, no. 1, pp. 180–187, Feb. 1988.
- [22] C. Concordia and S. Ihara, "Load representation in power system stability studies," *IEEE Trans. Power App. Syst.*, vol. PAS-101, no. 4, pp. 969–977, Apr. 1982.
- [23] P. Kundur, *Power System Stability and Control*. New York: McGraw-Hill, 1994, pp. 17–279.
- [24] J. R. Ribeiro and F. F. Lange, "A new aggregation method for determining composite load characteristics," *IEEE Trans. Power App. Syst.*, vol. PAS-101, no. 8, pp. 2869–2875, Aug. 1982.
- [25] "EPRI report load modeling for power flow and transient stability computer studies," New York, EPRI Final Rep. EL-5003, Jan. 1987, vol. 2.
- [26] D. Shmilovitz, J. Duan, D. Czarkowski, Z. Zabar, and S. Lee, "Characteristics of modern nonlinear loads and their influence on systems with distributed generation," *Int. J. Energy Technol. Policy*, vol. 5, no. 2, pp. 219–240, 2007.
- [27] M. Diaz-Aguilo, J. Sandraz, R. Macwan, F. d. León, D. Czarkowski, C. Comack, and D. Wang, "Field validated load model for the analysis of cvr in distribution secondary networks: Energy conservation," in *IEEE Trans. Power Del.*, accepted for publication.

Abdullah Bokhari (S'12) received the B.Sc. degree in electrical engineering from King Saud University, Riyadh, Saudi Arabia, in 2004 and the M.Sc. degree in electrical engineering from the Polytechnic Institute of New York University, Brooklyn, NY, USA, in 2009, where he is currently pursuing the Ph.D. degree in electrical engineering.

His research interests include power system modeling and analysis, power theory, and electrical machines.

Ali Alkan was born in Konya, Turkey. He received the B.Sc. degree in electrical and electronics engineering from TOBB University of Economics and Technology, Ankara, Turkey, in 2008 and the M.Sc. degree in electrical engineering from Polytechnic Institute of New York University, Brooklyn, NY, USA, in 2012.

Rasim Dogan received the B.Sc. degree in electrical and electronics engineering from Gazi University, Ankara, Turkey, the M.Sc. degree in electrical engineering from the Polytechnic Institute of New York University, Brooklyn, NY, USA, and is currently pursuing the Ph.D. degree in electrical engineering from Polytechnic Institute of New York University.

His research interests are power system load modeling and the calculation of electromagnetic fields applied to machine design.

Marc Diaz-Aguiló was born in Barcelona, Spain. He received the M.Sc. degree in telecommunications engineering from the Technical University of Catalonia (UPC), Barcelona, Spain, in 2006 and the M.Sc. degree in aerospace controls engineering from a joint program between Supaero, Toulouse France, and the Massachusetts Institute of Technology, Cambridge, MA USA, in 2008, and the Ph.D. degree in aerospace simulation and controls from the Technical University of Catalonia, Barcelona, Spain, in 2011.

Currently, he is a Postdoctoral Researcher at the Polytechnic Institute of New York University, Brooklyn, NY, USA. His research interests are in power systems, controls, smart-grid implementations, and large systems modeling and simulation.

Francisco de León (S'86–M'92–SM'02) received the B.Sc. and the M.Sc. (Hons.) degrees in electrical engineering from the National Polytechnic Institute, Mexico City, Mexico, in 1983 and 1986, respectively, and the Ph.D. degree in electrical engineering from the University of Toronto, Toronto, ON, Canada, in 1992.

He has held several academic positions in Mexico and has worked for the Canadian electric industry. Currently, he is an Associate Professor at the Polytechnic Institute of New York University, Brooklyn, NY, USA. His research interests include the analysis of power phenomena under nonsinusoidal conditions, the transient and steady-state analyses of power systems, the thermal rating of cables, and the calculation of electromagnetic fields applied to machine design and modeling.

Dariusz Czarkowski (M'97) received the M.Sc. degree in electronics from the AGH University of Science and Technology, Cracow, Poland, in 1989, the M.Sc. degree in electrical engineering from Wright State University, Dayton, OH, USA, in 1993, and the Ph.D. degree in electrical engineering from the University of Florida, Gainesville, FL, USA, in 1996.

In 1996, he joined the Polytechnic Institute of New York University, Brooklyn, NY, where he is currently an Associate Professor of Electrical and Computer Engineering. He is a coauthor of *Resonant Power Converters* (Wiley, 2011). His research interests are in the areas of power electronics, electric drives, and power quality.

Zivan Zabar (M'76–SM'81) was born in Hadera, Israel, in 1939. He received the B.Sc., M.Sc., and D.Sc. degrees in electric power and power electronics from Technion-Israel Institute of Technology, Haifa, Israel, in 1965, 1968, and 1972, respectively.

He is Professor of Electrical Engineering at the Polytechnic Institute of New York University, Brooklyn, NY, USA. He served as the Head of the Electrical and Computer Engineering Department, Polytechnic Institute of New York University, for three years (from 1995 to 1998). He has six patents and more than 50 papers published in technical journals. His areas of interest are electric power systems, electric drives, and power electronics.

Dr. Zabar is a member of Sigma Xi.

Leo Birenbaum (S'45–A'48–M'55–SM'70) was born in New York City in 1927. He received the B.E.E. degree from the Cooper Union, New York, USA, in 1946, and the M.E.E. and M.S. (Phys.) degrees from Polytechnic Institute, Brooklyn, NY, USA, in 1958 and 1974, respectively.

Currently, he is Professor Emeritus at the Polytechnic Institute, where, for many years, he taught courses in electric circuits, electromechanical power conversion, electromagnetic fields, and rotating machinery. He has conducted research in a number of areas: microwave components and transmission, biological effects of microwave and low-frequency electromagnetic fields, electromagnetic launchers, and electric power distribution. He is a coauthor of approximately 40 peer-reviewed papers, and he holds three patents on microwave devices.

Prof. Birenbaum is a member of Sigma Xi, Tau Beta Pi, the BioElectroMagnetics Society, and the New York Academy of Sciences.

Anthony Noel (M'81) was born in Brooklyn, NY, USA. He received the B.Sc. degree in electrical engineering from Columbia University, New York, USA, in 1981.

In 1993, he completed the General Electric Power Systems Engineering Course, General Electric, Schenectady, NY, USA. From 1982 to 2013, he was an Electrical Engineer with Consolidated Edison, New York, involved in distribution system planning and analysis. Presently he is an Asset Management Expert with Public Service Electric & Gas, Newark, NJ, USA.

Resk Ebrahem Uosef (M'01) received the B.Sc. and M.Sc. degrees in electrical engineering from Alexandria University Faculty of Engineering, Alexandria, Egypt, in 1979 and 1981, respectively, and a second M.Sc. degree in electrical engineering, and the Ph.D. degree in electrical engineering from Polytechnic University, Brooklyn, NY, USA, in 2007 and 2011, respectively.

He was an Engineer in a hydropower generating station in Egypt, and then he was the owner of a consulting firm for an electric construction company in Egypt. He joined Con Edison's Distribution Engineering Department, New York, USA, in 2003 and is currently responsible for Con Edison's distribution system design and analysis.

Dr. Uosef is a Registered Professional Engineer in the State of New York.